On the Statistical Resolution Limit (SRL) for Time-Reversal based MIMO radar

Messaoud Thameri, Karim Abed-Meraim, Foroohar Foroozan, Rémy Boyer, Amir Asif

PII: S0165-1684(17)30387-0
DOI: 10.1016/j.sigpro.2017.10.029
Reference: SIGPRO 6650

To appear in: *Signal Processing*

Received date: 8 May 2017
Revised date: 15 September 2017
Accepted date: 30 October 2017

Please cite this article as: Messaoud Thameri, Karim Abed-Meraim, Foroohar Foroozan, Rémy Boyer, Amir Asif, On the Statistical Resolution Limit (SRL) for Time-Reversal based MIMO radar, *Signal Processing* (2017), doi: 10.1016/j.sigpro.2017.10.029

Highlights

- At first, we derive the theoretical SRL expressions for the TR-MIMO and conventional MIMO radar systems;
- Contrary to existing works, we take into account all the noise terms and particularly the required noise whitening process for the exact SRL formula computation;
- Finally, we provide a performance comparison between the conventional and TR schemes which confirms the performance gain shown in the literature (e.g. Foroozan et al (2013)) when the noise term of the time reversed signal is neglected. However, our analysis highlights the fact that the TR scheme's gain would be lost in the case where such assumption is not any more valid.

On the Statistical Resolution Limit (SRL) for Time-Reversal based MIMO radar

Messaoud THAMERI[a,*], Karim Abed-Meraim[b], Foroohar Foroozan[c], Rémy Boyer[d], Amir Asif[e]

[a] *École Supérieur Ali CHABATI, Algiers, Algeria*
[b] *PRISME Laboratory, Polytech'Orléans, Orléans University, France.*
[c] *InnoMind Technology Corporation, Toronto, Canada*
[d] *University of Paris-Sud, Laboratoire des Signaux et Systèmes (L2S lab.), Gif-Sur-Yvette, France*
[e] *Concordia University, Montreal, Canada*

Abstract

In the single-input multiple-output radar, the system transmits scaled (coherent) versions of a single waveform. The multiple-input multiple-output (MIMO) radar uses multiple antennas to simultaneously transmit several non-coherent waveforms and exploits multiple antennas to receive the reflected signals (echoes). This diversity in term of waveform coding allows to transmit orthogonal waveforms which enables the MIMO radar superiority in several fundamental aspects, including: improved parameter identifiability and estimation and much enhanced flexibility for transmit beam-pattern design. The context of this work is the co-located MIMO radar where the transmit and the receive arrays are close in space. In this paper, we provide a theoretical performance analysis to compare two configurations of MIMO radar: conventional configuration and Time Reversal (TR) configuration in term of Statistical Resolution Limit (SRL). This study provides new insights on the performance gain of the TR scheme which is discussed and illustrated by appropriate simulation results depending on the receive noise level.

Keywords: Cramér-Rao Bound, Statistical Resolution Limit, Source detection and localization, MIMO radar, Time Reversal.

*Corresponding author

1. Introduction

In the Time Reversal (TR) communication scheme, several pulses, transmitted through a dispersive medium, are received by an array, then time reversed, energy normalized, and retransmitted through the same channel. If the scattering channel is reciprocal[1], the retransmitted waveform refocuses on the original source. Recently, the TR strategy has been successively exploited for source localization [1] in the sense that the Directions of Arrival (DOA) of the sources are estimated with higher accuracy as compared to the conventional approach (without TR strategy). In the context of (Multipe-Input Multiple-Output) MIMO radar, the new scheme is denoted by the acronym TR-MIMO radar. The TR-MIMO radar benefits from (*i*) an extra degree of freedom and increased design flexibility, e.g. [2, 3], due to the MIMO strategy and (*ii*) the focusing property of the TR approach. As shown in [4], the target detection performance is improved for a TR-MIMO radar.

Regarding the theoretical performance of any system, it is interesting to consider lower bound of the MSE (Mean Squared Error) as the Cramer-Rao Bound (CRB) and the related resolution capability, namely the Statistical Resolution Limit (SRL) [5, 6]. The CRB and the SRL, denoted by δ, are useful as a touchstone against which the efficiency of the considered estimators can be tested. The SRL can be interpreted as the minimal separation in the parameter set to resolve two closely spaced targets as illustrated in Fig. 1.

The evaluation of the resolution limit is an old and fundamental problem and a survey can be found in references [5, 6]. In [7], it is shown that the SRL is the solution of an equation involving the CRB of the SRL given by $\delta^2 =$

[1]Due to the reciprocity principle, the forward and reverse channels are assumed to be the same.

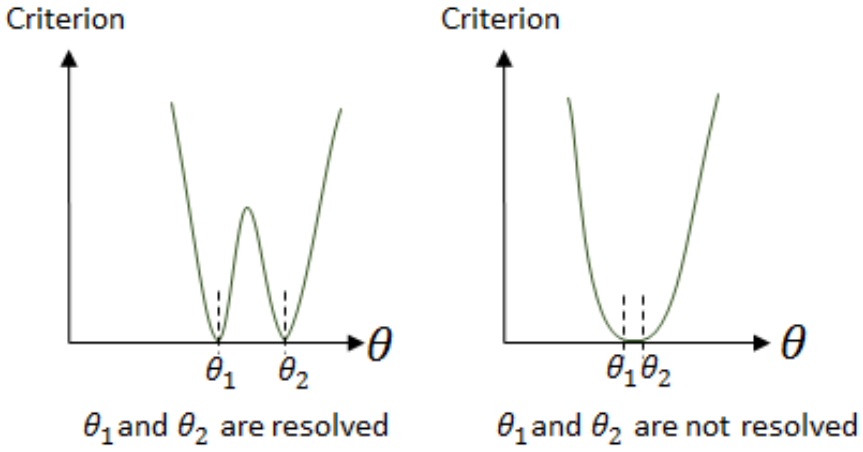

Figure 1: Resolution of two closely spaced parameters

μCRB(δ) where $\mu > 0$ is a properly chosen scalar factor. In addition, in [8], it is demonstrated that this equation naturally appears in the performance of the Generalized Likelihood Ratio Test (GLRT) for a binary hypothesis test consisting of the decision between the presence of one or two targets. Hence, the criterion introduced heuristically in [7] is in fact optimal in the sense it coincides with the GLRT. In our work, it is this second strategy based on the GLRT that is adopted due to its relative simplicity in the considered context. The CRB and the SRL for the co-located MIMO radar (without TR) are derived and analysed in [9]. In [10], the CRB and the SRL are derived for the TR-MIMO and the gain to use the TR strategy at high Signal to Noise Ratio (SNR) is demonstrated. On the other hand, in [11], it is shown that an other interesting quantity to assess the performance of a MIMO system is to derive the minimal theoretical SNR in order to resolve two closely spaced targets. This SNR is shown to be a quadratic function of the inverse SRL value. In this paper, we extend the work initiated in [11] for the MIMO radar to the TR-MIMO radar context.

More precisely, our contributions are threefold: (i) at first we derive the theoretical SRL expressions for the TR-MIMO and conventional MIMO cases;

(ii) contrary to existing works, we take into account all the noise terms and particularly the required noise whitening process for the exact SRL formula computation; (iii) finally, we provide a performance comparison between the conventional and TR schemes which confirms the performance gain shown in [10, 4] when the noise term of the time reversed signal is neglected. However, our analysis highlights the fact that the TR scheme's gain would be lost in the case where such assumption is not any more valid. This result is well aligned with the general observation made in [12] about the TR scheme.

The rest of the paper is organised as follows: Section 2 gives the mathematical model in conventional and TR MIMO radar. Taylor expansion w.r.t. the SRL is presented in section 3 while the formulation of the hypothesis test is given by section 4. Section 5 presents expressions of the SRL as well as the minimum SNR needed to resolve two closely space sources. Numerical simulations and discussions are presented in section 6. Finally, the conclusion of presented work is given is section 7.

2. Model setup for Conventional and TR MIMO radar

We consider two co-located arrays A and B (with P and N sensors respectively as shown in Fig. 2). First, array A sends to array B a $(P \times 1)$ wideband signal vector $\mathbf{f}_A(t)$, with carrier frequency ω_c. Secondly, array B sends to array A another $(N \times 1)$ wideband signal vector $\beta \mathbf{f}_B(t)$, with the same carrier frequency ω_c and $\beta = \sqrt{\frac{E_{\mathbf{f}_A}}{E_{\mathbf{f}_B}}}$ being a normalization constant. Here, $E_{\mathbf{f}_B}$ (resp. $E_{\mathbf{f}_A}$) stands for the energy of transmitted signal (resp. the energy of received signal), assuming that all the antennas in A and B are transmitting with the same power. In the following sections 2.1 and 2.2, we derive the expression of the first set of observations at array B in the single source and multiple sources cases, respectively. Then, in the same way, we will deduce the second set of observations at array A in section 2.3. Finally, the model setup for the TR-MIMO radar is provided in subsection 2.4.

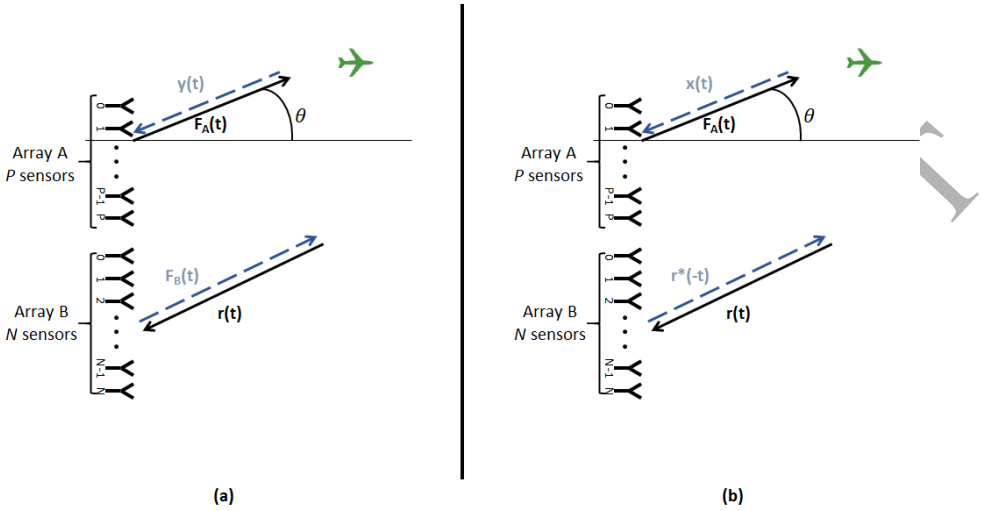

Figure 2: Propagation model: (a) Conventional model. (b) Time Reversal model. Clutter and scatterer signals are not presented.

2.1. Single source case

To formulate our model's equation, we assume at first that the emitted signals illuminate only one source. The observed signal at the n^{th} sensor of array B is expressed as:

$$[\mathbf{r}(t)]_n = \sum_{p=1}^{P} \alpha_{np} \left[\mathbf{f}_A(t - \tilde{\tau}_p^A - \tilde{\tau}_n^B)\right]_p + [\mathbf{v}(t)]_n + [\mathbf{r}_a(t)]_n \,. \tag{1}$$

where $[.]_n$ stands for the n^{th} component, and α_{np} is the attenuation associated to the considered source when sensor p is probing and sensor n is receiving. The target is assumed to be in the far field of the co-located arrays so that the attenuation $\alpha_{np} = \alpha$ for all n, p. Let $\tilde{\tau}_p^A = \frac{r_0}{c} + \tau_p^A(\Omega)$, $\tilde{\tau}_n^B = \frac{r_0}{c} + \tau_n^B(\Omega)$, where r_0 is the range of the target w.r.t. the reference sensor, $\tau_p^A(\Omega)$ (resp. $\tau_n^B(\Omega)$) stands for the time delay of the p^{th} sensor of the array A (resp. n^{th} sensor of the array B) w.r.t. the sensor reference which depends[2] on $\Omega = sin(\theta)$, where

[2]The expression of these delays are given in the sequel for uniform linear array geometry.

θ is the direction of arrival (DOA) of the source signal. The additive noise $\mathbf{v}(t)$ is a white circular Gaussian process with zero mean and variance σ_v^2 and $\mathbf{r}_a(t)$ represents the clutter response. In the following and similarly to [13, 8], we assume that the clutter signal is known (or previously estimated) and then it will be removed from the considered model.

The frequency component of (1) in the q^{th} frequency bin (denoted ω_q) can be expressed as (the signals are down converted to baseband)

$$[\mathbf{r}(\omega_q)]_n = \alpha \sum_{p=1}^{P} e^{-j(\omega_q+\omega_c)\left(\frac{2r_0}{c}+\tau_p^A(\Omega)+\tau_n^B(\Omega)\right)} [\mathbf{f}_A(\omega_q)]_p + [\mathbf{v}(\omega_q)]_n. \quad (2)$$

The observed vector in matrix form is given by

$$\mathbf{r}(\omega_q) = \alpha e^{-j(\omega_q+\omega_c)\frac{2r_0}{c}} \mathbf{A}(\Omega,\omega_q)\mathbf{f}_A(\omega_q) + \mathbf{v}(\omega_q). \quad (3)$$

where the $(n,p)^{th}$ element of the transmit-receive propagation matrix $\mathbf{A}(\Omega,\omega_q)$ is given by $[\mathbf{A}(\Omega,\omega_q)]_{np} = e^{-j(\omega_q+\omega_c)(\tau_n^B(\Omega)+\tau_p^A(\Omega))}$, $1 \le n \le N$ and $1 \le p \le P$.

2.2. Multiple sources case

Now, we generalize equation (3) to the multiple sources context, in which case we have

$$\mathbf{r}(\omega_q) = \sum_{l=1}^{L} \mathbf{A}_l(\Omega_l,\omega_q)\mathbf{f}_A(\omega_q) + \mathbf{v}(\omega_q). \quad (4)$$

where $\mathbf{A}_l(\Omega_l,\omega_q) = \alpha_l e^{-j(\omega_q+\omega_c)\frac{2r_{0_l}}{c}} \mathbf{A}(\Omega_l,\omega_q)$, $1 \le l \le L$ and L is the number of sources.

Let $\mathbf{r} = \left[\mathbf{r}^T(\omega_1),\cdots,\mathbf{r}^T(\omega_Q)\right]^T$ be the vector of size $(NQ\times 1)$ of all frequency components. It can be expressed as

$$\mathbf{r} = \sum_{l=1}^{L} \mathbf{A}_l(\Omega_l)\mathbf{f}_A + \mathbf{v}. \quad (5)$$

where $\mathbf{A}_l(\Omega_l) = Bdiag\left[\mathbf{A}_l(\Omega_l,\omega_1),\cdots,\mathbf{A}_l(\Omega_l,\omega_Q)\right]$, $Bdiag$ stands for 'Block diag' operator, $\mathbf{f}_A = \left[\mathbf{f}_A^T(\omega_1),\cdots,\mathbf{f}_A^T(\omega_Q)\right]^T$ and $\mathbf{v} = \left[\mathbf{v}^T(\omega_1),\cdots,\mathbf{v}^T(\omega_Q)\right]^T$.

2.3. Retransmitted signals from array B to array A

In the same way as previous subsections, the second set of observations in the q^{th} frequency bin ω_q is given by

$$\mathbf{y}(\omega_q) = \beta_c \sum_{l=1}^{L} \mathbf{A}_l^T(\Omega_l, \omega_q)\mathbf{f}_B(\omega_q) + \mathbf{w}(\omega_q). \tag{6}$$

where $\beta_c = \sqrt{\frac{E_{\mathbf{f}_A}}{E_{\mathbf{f}_B}}}$ is a power normalizing factor ($\mathbf{E}_{\mathbf{f}_A}$ and $\mathbf{E}_{\mathbf{f}_B}$ being the energy used by array A and B respectively), $\mathbf{w}$ is white circular Gaussian noise with zero mean and variance σ_w^2. The $(PQ \times 1)$ observation vector $\mathbf{y}$ can be expressed as

$$\mathbf{y} = \beta_c \sum_{l=1}^{L} \mathbf{A}_l^T(\Omega_l)\mathbf{f}_B + \mathbf{w}. \tag{7}$$

where $\mathbf{f}_B = [\mathbf{f}_B(\omega_1), \cdots, \mathbf{f}_B(\omega_Q)]^T$ and $\mathbf{w}_B = [\mathbf{w}_B(\omega_1), \cdots, \mathbf{w}_B(\omega_Q)]^T$. In (7), we have assumed a symmetric channel so that if $\mathbf{A}_l(\Omega_l)$ models the transmission from A to B then $\mathbf{A}_l^T(\Omega_l)$ represents the propagation channel from B to A. Finally, the data in $\mathbf{r}$ and $\mathbf{y}$ are both concatenated to form the total observation vector $\mathbf{u}_c$ according to:

$$\mathbf{u}_c = \begin{bmatrix} \mathbf{r}^T & \mathbf{y}^T \end{bmatrix}^T. \tag{8}$$

2.4. Model setup for Time Reversal observations

Now we consider the TR case where array A sends a wideband signal $\mathbf{f}_A$, with carrier frequency ω_c. The observed data at B (i.e., $\mathbf{r}$ in equation (5)) is recorded, energy normalized, time reversed (TR) and retransmitted (i.e., we transmit $\beta_{TR}\mathbf{r}(-t)$ where $\beta_{TR} = \sqrt{\frac{E_{\mathbf{f}_A}}{E_{\mathbf{f}_B}}}$). Based on equation (6), the received vector $\mathbf{x}$ at array A is given by

$$\begin{aligned} \mathbf{x}(\omega_q) &= \beta_{TR} \sum_{l=1}^{L} \mathbf{A}_l^T(\Omega_l, \omega_q)\mathbf{r}^*(\omega_q) + \mathbf{w}(\omega_q), \\ &= \beta_{TR} \left(\sum_{l=1}^{L} \mathbf{A}_l^T(\Omega_l, \omega_q) \sum_{l'=1}^{L} \mathbf{A}_{l'}^*(\Omega_l^{'}, \omega_q) \right) \mathbf{f}_A^*(\omega_q) + \mathbf{n}^{'}(\omega_q). \end{aligned} \tag{9}$$

where $\mathbf{n}^{'}(\omega_q) = \beta_{TR}\sum_{l=1}^{L}\mathbf{A}_l^T(\Omega_l)\mathbf{v}^*(\omega_q) + \mathbf{w}(\omega_q)$. The $(PQ \times 1)$ observation vector $\mathbf{x}$ can be expressed as

$$\mathbf{x} = \beta_{TR}\left(\sum_{l=1}^{L}\mathbf{A}_l^T(\Omega_l)\sum_{l'=1}^{L}\mathbf{A}_{l'}^*(\Omega_l^{'})\right)\mathbf{f}_A^* + \mathbf{n}^{'}. \tag{10}$$

where $\mathbf{n}^{'} = \left[\mathbf{n}^{'T}(\omega_1), \ \cdots, \ \mathbf{n}^{'T}(\omega_q)\right]^T$. Now, the TR observations set is formed using $\mathbf{r}$ and $\mathbf{x}$ as

$$\mathbf{u}_{TR} = \left[\mathbf{r}^T \ \ \mathbf{x}^T\right]^T. \tag{11}$$

3. Taylor expansion and linear model w.r.t. SRL

In the sequel, we consider the situation where two sources are closely spaced in terms of DOA while the other sources (if any) are far away with known (or well estimated) parameters. Following the methodology introduced in [14], the aim of this section is to linearise, w.r.t. the angle difference of two closely spaced sources, equations (5) and (7) (i.e., conventional model) and (10) (i.e., TR model) using Taylor expansion. The result will be used to derive the minimum Signal to Noise Ratio (SNR) required to resolve the considered two closely space sources. Without loss of generality, we consider that these two sources are parametrized by Ω_1 and Ω_2, in which case we denote by $\delta = \Omega_2 - \Omega_1$ the 'distance' between the two parameters and by $\Omega_c = \frac{\Omega_1+\Omega_2}{2}$ their center.

For simplicity, we consider next two aligned uniform arrays (A and B) as shown in Fig. 2, for which the resolution limit is developed. in that case the time delays expressions are given by

$$\tau_n^B(\Omega) = \frac{d_n^B}{c}\Omega \tag{12}$$

$$\tau_p^A(\Omega) = \frac{d_p^A}{c}\Omega \tag{13}$$

where d_n^B (resp. d_p^A) is the distance between the n^{th} sensor of the array B (resp. p^{th} sensor of the array A) and the reference sensor.

3.1. Conventional model

As shown in Appendix A, the first-order Taylor expansion of (5) around $\delta = 0$ leads to

$$\mathbf{r} \overset{1}{\approx} \mathbf{A}_c \mathbf{f}_A + \delta \mathbf{D} \mathbf{f}_A + \sum_{l=3}^{L} \mathbf{A}_l(\Omega_l)\mathbf{f}_A + \mathbf{v}. \tag{14}$$

where $\overset{1}{\approx}$ means the first-order approximation and

$$\mathbf{A}_c = Bdiag\left[\mathbf{A}_c(\omega_1), \cdots, \mathbf{A}_c(\omega_Q)\right], \tag{15}$$

$$\mathbf{D} = Bdiag\left[\mathbf{D}(\omega_1), \cdots, \mathbf{D}(\omega_Q)\right]. \tag{16}$$

The $(n,p)^{th}$ element of matrices $\mathbf{A}_c(\omega_q)$ and $\mathbf{D}(\omega_q)$ are given by

$$\left[\mathbf{A}_c(\omega_q)\right]_{np} = \alpha_+(\omega_q) e^{-j\frac{(\omega_q+\omega_c)(d_n^B + d_p^A)}{c}\Omega_c}, \tag{17}$$

$$\left[\mathbf{D}(\omega_q)\right]_{np} = \alpha_-(\omega_q) j \frac{(\omega_q+\omega_c)(d_n^B + d_p^A)}{2c} e^{-j\frac{(\omega_q+\omega_c)(d_n^B + d_p^A)}{c}\Omega_c}, \tag{18}$$

with

$$\alpha_+(\omega_q) = \alpha_1 e^{-j(\omega_q+\omega_c)\frac{2r_{0_1}}{c}} + \alpha_2 e^{-j(\omega_q+\omega_c)\frac{2r_{0_2}}{c}}, \tag{19}$$

$$\alpha_-(\omega_q) = \alpha_1 e^{-j(\omega_q+\omega_c)\frac{2r_{0_1}}{c}} - \alpha_2 e^{-j(\omega_q+\omega_c)\frac{2r_{0_2}}{c}}. \tag{20}$$

In the same way, The first-order Taylor expansion around $\delta = 0$ of (7) leads to

$$\mathbf{y} \overset{1}{\approx} \beta_c \mathbf{A}_c^T \mathbf{f}_B + \delta \beta_c \mathbf{D}^T \mathbf{f}_B + \beta_c \sum_{l=3}^{L} \mathbf{A}_l^T(\Omega_l)\mathbf{f}_B + \mathbf{w}. \tag{21}$$

The first-order Taylor expansion of the conventional data set $\mathbf{u}_c$ (cf. equation (8)) is given by

$$\mathbf{u}_c \overset{1}{\approx} \mathbb{A}_c \mathbf{f}_c + \delta \mathbb{D}_c \mathbf{f}_c + \sum_{l=3}^{L} \mathbb{A}_l(\Omega_l)\mathbf{f}_c + \xi_c. \tag{22}$$

where $\mathbb{A}_c = Bdiag\left[\mathbf{A}_c, \beta_c \mathbf{A}_c^T\right]$, $\mathbb{D}_c = Bdiag\left[\mathbf{D}, \beta_c \mathbf{D}^T\right]$, $\mathbb{A}_l(\Omega_l) = Bdiag\left[\mathbf{A}_l(\Omega_l), \beta_c \mathbf{A}_l^T(\Omega_l)\right]$ $\mathbf{f}_c = \left[\mathbf{f}_A^T, \mathbf{f}_B^T\right]^T$ and $\xi_c = \left[\mathbf{v}^T, \mathbf{w}^T\right]^T$.

3.2. Time Reversal model

As shown in Appendix B, the first-order Taylor expansion of (10) around $\delta = 0$ leads to

$$\mathbf{x} \overset{1}{\approx} \beta_{TR}\mathbf{H}_c\mathbf{f}_A^* + \beta_{TR}\delta\mathbf{H}_d\mathbf{f}_A^* + \beta_{TR}\delta\mathbf{D}^T\mathbf{v}^* + \mathbf{w}^{'}. \tag{23}$$

where

$$\begin{aligned}
\mathbf{H}_c &= Bdiag\left[\mathbf{H}_c(\omega_1), \cdots, \mathbf{H}_c(\omega_Q)\right], && (24)\\
\mathbf{H}_d &= Bdiag\left[\mathbf{H}_d(\omega_1), \cdots, \mathbf{H}_d(\omega_Q)\right], && (25)\\
\mathbf{A}_{cc}(\omega_q) &= \mathbf{A}_c(\omega_q) + \sum_{l=3}^{L}\mathbf{A}_l(\Omega_l, \omega_q),\\
\mathbf{H}_c(\omega_q) &= \mathbf{A}_{cc}^T(\omega_q)\mathbf{A}_{cc}^*(\omega_q),\\
\mathbf{H}_d(\omega_q) &= \mathbf{A}_{cc}^T(\omega_q)\mathbf{D}^*(\omega_q) + \mathbf{D}^T(\omega_q)\mathbf{A}_{cc}^*(\omega_q),\\
\mathbf{w}^{'} &= \left[\mathbf{w}^{'T}(\omega_1), \ \cdots, \ \mathbf{w}^{'T}(\omega_q)\right]^T, && (26)\\
\mathbf{w}^{'}(\omega_q) &= \beta_{TR}\mathbf{A}_{cc}(\omega_q)\mathbf{v}^*(\omega_q) + \mathbf{w}(\omega_q).
\end{aligned}$$

One can observe that the noise term $\left(\beta_{TR}\delta\mathbf{D}^T\mathbf{v}^* + \mathbf{w}^{'}\right)$ is not white anymore[3]. For that and in order to simplify the computation of the SINR, we whiten the observed vector $\mathbf{x}$. As shown in Appendix C, the whitened vector $\tilde{\mathbf{x}}$ is given by

$$\tilde{\mathbf{x}} = \beta_{TR}\mathbf{W}_0\mathbf{H}_c\mathbf{f}_A^* + \beta_{TR}\delta\left(\mathbf{W}_0\mathbf{H}_d - \frac{\beta_{TR}^2\sigma_{\mathbf{v}}^2}{2\sigma^2}\mathbf{W}_0^{\frac{3}{2}}\mathbf{H}_d\mathbf{W}_0^{\frac{3}{2}}\mathbf{H}_c\right)\mathbf{f}_A^* + \mathbf{v}'. \tag{27}$$

where $\mathbf{W}_0 = Bdiag\left[\mathbf{W}_0(\omega_1), \cdots, \mathbf{W}_0(\omega_Q)\right]$ and $\mathbf{W}_0(\omega_q) = \sigma\mathbf{R}_0^{-\frac{1}{2}}(\omega_q)$ is the principal term of the first order expansion of the whitening matrix (see Appendix Appendix C for details), with $\mathbf{R}_0(\omega_q)$ is the covariance matrix of $\mathbf{x}(\omega_q)$ for $\delta = 0$, $\left(\mathbf{R}_0(\omega_q) = \beta_{TR}^2\sigma_{\mathbf{v}}^2\mathbf{H}_c(\omega_q) + \sigma_{\mathbf{w}}^2\mathbf{I}\right)$, and $\mathbf{v}' \sim CN(\mathbf{0}, \sigma^2\mathbf{I})$.

[3]The noise $\left(\beta_{TR}\delta\mathbf{D}^T\mathbf{v}^*(\omega_q) + \mathbf{w}^{'}(\omega_q)\right) \sim CN\left(0, \mathbf{R}_\delta(\omega_q)\right)$, where $\mathbf{R}_\delta(\omega_q) = \beta_{TR}^2\sigma_{\mathbf{v}}^2\left(\mathbf{H}_c(\omega_q) + \delta\mathbf{H}_d(\omega_q)\right) + \sigma_{\mathbf{w}}^2\mathbf{I}$, the term proportional to δ^2 is neglected here. For more details see Appendix C.

The first-order Taylor expansion of the TR data vector $\mathbf{u}_{TR}$ is given by

$$\mathbf{u}_{TR} \overset{1}{\approx} \mathbb{A}_{TR}\mathbf{f}_{TR} + \delta\mathbb{D}_{TR}\mathbf{f}_{TR} + \sum_{l=3}^{L} \mathbb{O}_l(\Omega_l)\mathbf{f}_{TR} + \xi_{TR}. \tag{28}$$

where $\mathbb{A}_{TR} = Bdiag\left[\mathbf{A}_c, \beta_{TR}\mathbf{W}_0\mathbf{H}_c\right]$, $\mathbb{D}_{TR} = Bdiag\left[\mathbf{D}, \beta_{TR}\left(\mathbf{W}_0\mathbf{H}_d - \frac{\beta_{TR}^2\sigma_v^2}{2\sigma^2}\mathbf{W}_0^{\frac{3}{2}}\mathbf{H}_d\mathbf{W}_0^{\frac{3}{2}}\mathbf{H}_c\right)\right]$, $\mathbb{O}_l(\Omega_l) = Bdiag\left[\mathbf{A}_l(\Omega_l), \mathbf{0}_{QP\times QP}\right]$, all the elements of the matrix $\mathbf{0}$ are equal to 0, $\mathbf{f}_{TR} = \left[\mathbf{f}_A^T, \mathbf{f}_A^H\right]^T$ and $\xi_{TR} = \left[\mathbf{v}^T, \mathbf{v}'^T\right]^T$.

4. Hypothesis test formulation

In the following we assume that two sources are in the vicinity of each other. Let the hypothesis $\mathcal{H}_0$ represents the case where the two Source Of Interest (SOI) exist but are combined into a single signal, whereas the hypothesis $\mathcal{H}_1$ embodies the situation where the two SOI are resolvable. Consequently, a convenient binary hypothesis test is given by

$$\begin{cases} \mathcal{H}_0 : \ \delta = 0 \\ \mathcal{H}_1 : \ \delta \neq 0 \end{cases} \tag{29}$$

In this case, the Generalized Likelihood Ratio Test [15] is given by

$$G(\mathbf{u}) = \frac{p(\mathbf{u}; \hat{\delta}, \mathcal{H}_1)}{p(\mathbf{u}; \mathcal{H}_0)} \underset{\mathcal{H}_1}{\overset{\mathcal{H}_0}{\lessgtr}} \eta'. \tag{30}$$

in which $p(\mathbf{u}; \mathcal{H}_0)$ and $p(\mathbf{u}; \mathcal{H}_1)$ denote the probability density functions (pdf) under $\mathcal{H}_0$ and $\mathcal{H}_1$, respectively, and where η', $\hat{\delta}$ denote the detection threshold, the maximum likelihood estimate (MLE) of δ under $\mathcal{H}_1$. If the statistic $G(\mathbf{u})$ is greater than a given threshold η', then the signals are said to be resolvable.

In the following, we assume that Ω_c and $\mathbf{A}_l(\Omega_l)$, $3 \leq l \leq L$ are known or previously estimated. This simplifying assumption can be justified as follows:

- The directions of arrival as well as the cross section coefficients of well separated sources (i.e. sources 3 to L) can be accurately estimated and hence, for simplicity, they are assumed known in the sequel. This is also the case for the central direction Ω_c of the two closely spaced sources.

- Note that simplifying assumptions are often used when deriving the performance bounds due to the problem difficulty. For this reason, most papers investigating the estimation performance bounds (Cramer Rao Bounds or others) rely on the simplifying assumption that the detection of the number of sources is perfect and focus only on the estimation performance bound. Similarly, in our case, we assume that the estimation of the previously mentioned parameters is perfect and focus only on the detection performance bound. This allows us to understand how the SRL depends on different system parameters including the SNR, the number of sensors and their location, the unknown cross section coefficients of the two closely spaced sources, the waveform signal, etc. and to compare the two considered schemes (with or without the TR).

We define now new observation vectors: $\mathbf{z}_c$ for the conventional model

$$\begin{aligned} \mathbf{z}_c &= \mathbf{u}_c - \mathbb{A}_c\mathbf{f}_c - \sum_{l=3}^{L}\mathbb{A}_l(\Omega_l)\mathbf{f}_c, \\ &= \delta\mathbb{D}_c\mathbf{f}_c + \xi_c, \end{aligned} \tag{31}$$

and $\mathbf{z}_{TR}$ for the time reversal model

$$\begin{aligned} \mathbf{z}_{TR} &= \mathbf{u}_{TR} - \mathbb{A}_{TR}\mathbf{f}_{TR} - \sum_{l=3}^{L}\mathbb{O}_l(\Omega_l)\mathbf{f}_{TR}, \\ &= \delta\mathbb{D}_{TR}\mathbf{f}_{TR} + \xi_{TR}. \end{aligned} \tag{32}$$

Without loss of generality, we define only one new observation vector $\mathbf{z}$

$$\mathbf{z} = \delta\mathbb{D}\mathbf{f} + \xi. \tag{33}$$

where $\mathbb{D} = \mathbb{D}_c$, $\mathbf{f} = \mathbf{f}_c$ and $\xi = \xi_c$ for the conventional model and $\mathbb{D} = \mathbb{D}_{TR}$, $\mathbf{f} = \mathbf{f}_{TR}$ and $\xi = \xi_{TR}$ for the time reversal model.

4.1. Binary hypothesis test

The binary hypothesis test for signal (33) is

$$\begin{cases} \mathcal{H}_0 : & \mathbf{z} = \xi \sim CN(0, \mathbf{R}_\xi) \\ \mathcal{H}_1 : & \mathbf{z} = \delta\mathbf{g} + \xi \sim CN(\delta\mathbf{g}, \mathbf{R}_\xi) \end{cases} \tag{34}$$

$$\text{where} \begin{cases} \mathbf{g} = \mathbb{D}_c \mathbf{f}_c \quad \text{and} \quad \mathbf{R}_\xi = Bdiag\left[\sigma_{\mathbf{v}}^2 \mathbf{I}, \sigma_{\mathbf{w}}^2 \mathbf{I}\right] & \text{for conventional model} \\ \mathbf{g} = \mathbb{D}_{TR} \mathbf{f}_{TR} \quad \text{and} \quad \mathbf{R}_\xi = Bdiag\left[\sigma_{\mathbf{v}}^2 \mathbf{I}, \sigma^2 \mathbf{I}\right] & \text{for time reversal model} \end{cases}$$

4.2. Constrained MLE (CMLE)

As the SRL δ is a real value, one has to define the constrained MLE (CMLE) of δ. More precisely, the constrained optimization problem can be written according to $\arg\min_\delta L(\mathbf{z}, \delta)$ subject to δ is real valued, where $L(\mathbf{z}, \delta)$ is the negative log-likelihood function is given by

$$\begin{aligned} L(\mathbf{z}, \delta) &= -ln(p(\mathbf{z})), & (35) \\ &= Q(N+P)\ln(\pi) + QN\ln(\sigma_N^2) + QP\ln(\sigma_P^2) \\ &+ \frac{1}{\sigma_N^2}\left\|\mathbf{z}_N - \delta \mathbf{g}_N\right\|^2 + \frac{1}{\sigma_P^2}\left\|\mathbf{z}_P - \delta \mathbf{g}_P\right\|^2. & (36) \end{aligned}$$

where $\mathbf{z} = [\mathbf{z}_N,\ \mathbf{z}_P]^T$, $\mathbf{z}_N = \left[z_{(1)}, \cdots, z_{(QN)}\right]^T$, $\mathbf{z}_P = \left[z_{(QN+1)}, \cdots, z_{(QN+QP)}\right]^T$, $\mathbf{g} = [\mathbf{g}_N,\ \mathbf{g}_P]^T$, $\mathbf{g}_N = \left[g_{(1)}, \cdots, g_{(QN)}\right]^T$ and $\mathbf{g}_P = \left[g_{(QN+1)}, \cdots, g_{(QN+QP)}\right]^T$, σ_N^2 and σ_P^2 are the noise variances associated to the observed vectors $\mathbf{z}_N$ and $\mathbf{z}_P$ respectively. In conventional case $(\sigma_N^2, \sigma_P^2) = (\sigma_{\mathbf{v}}^2, \sigma_{\mathbf{w}}^2)$ and in time reversal case $(\sigma_N^2, \sigma_P^2) = (\sigma_{\mathbf{v}}^2, \sigma^2)$.

This problem of optimization can be solved by the Lagrange multiplier method. The Lagrange function is given by

$$\mathcal{L}(\mathbf{z}, \delta) = L(\mathbf{z}, \delta) + \vartheta \Im(\delta). \quad (37)$$

where ϑ is a real Lagrange multiplier and $\Im(\delta)$ stands for the imaginary part of δ. The partial derivatives of the Lagrange function are

$$\begin{cases} \frac{\partial \mathcal{L}(\mathbf{z},\delta)}{\partial \delta} = \frac{1}{\sigma_N^2}\left(\left\|\mathbf{g}_N\right\|^2 \delta^* - \mathbf{z}_N^H \mathbf{g}_N\right) + \frac{1}{\sigma_P^2}\left(\left\|\mathbf{g}_P\right\|^2 \delta^* - \mathbf{z}_P^H \mathbf{g}_P\right) - \jmath\frac{\vartheta}{2} \\ \frac{\partial \mathcal{L}(\mathbf{z},\delta)}{\partial \vartheta} = \Im(\delta) \end{cases} \quad (38)$$

where the condition $\Im(\delta) = 0$ can be written according to $\jmath\frac{1}{2}(\delta - \delta^*) = 0$. By letting $\left.\frac{\partial \mathcal{L}(\mathbf{z},\delta)}{\partial \vartheta}\right|_{\vartheta=\vartheta_0} = 0$, one can obtain $\vartheta_0 = 2\Im\left(\frac{1}{\sigma_N^2}\mathbf{g}_N^H \mathbf{z}_N + \frac{1}{\sigma_P^2}\mathbf{g}_P^H \mathbf{z}_P\right)$. By replacing this expression in δ_0 expression obtained by letting $\left.\frac{\partial \mathcal{L}(\mathbf{z},\delta)}{\partial \delta}\right|_{\delta=\delta_0} = 0$, one obtains

$$\delta_0 = \frac{\sigma_N^2 \sigma_P^2}{\sigma_N^2\left\|\mathbf{g}_P\right\|^2 + \sigma_P^2\left\|\mathbf{g}_N\right\|^2} \Re\left(\frac{1}{\sigma_N^2}\mathbf{g}_N^H \mathbf{z}_N + \frac{1}{\sigma_P^2}\mathbf{g}_P^H \mathbf{z}_P\right) \quad (39)$$

Using (39), the statistic of the GLRT is then given by

$$G(\mathbf{z}) = \frac{p(\mathbf{z};\hat{\delta_0},\mathcal{H}_1)}{p(\mathbf{z};\mathcal{H}_0)} \underset{\mathcal{H}_1}{\overset{\mathcal{H}_0}{\lessgtr}} \eta', \tag{40}$$

$$= e^{\left\{\frac{1}{2\sigma_N^2}\left(\|\mathbf{z}_N\|^2-\|\mathbf{z}_N-\delta_0\mathbf{g}_N\|^2\right)+\frac{1}{2\sigma_P^2}\left(\|\mathbf{z}_P\|^2-\|\mathbf{z}_P-\delta_0\mathbf{g}_P\|^2\right)\right\}}. \tag{41}$$

Plugging (39) in (41) and defining a new statistic $\mathbf{T}(\mathbf{z})$, one obtains

$$\mathbf{T}(\mathbf{z}) = 2\ln(G(\mathbf{z})) \tag{42}$$

$$= \frac{\sigma_N^2\sigma_P^2}{\sigma_N^2\|\mathbf{g}_P\|^2+\sigma_P^2\|\mathbf{g}_N\|^2}\Re^2\left(\frac{1}{\sigma_N^2}\mathbf{g}_N^H\mathbf{z}_N+\frac{1}{\sigma_P^2}\mathbf{g}_P^H\mathbf{z}_P\right) \tag{43}$$

Using the result of Appendix D, we have

$$\mathbf{T}(\mathbf{z}) \sim \begin{cases} \chi_1^2 & \text{under } \mathcal{H}_0, \\ \chi_1^2(\lambda) & \text{under } \mathcal{H}_1. \end{cases} \tag{44}$$

where the non-centrality parameter is given by

$$\lambda = 2\delta_0^2\left(\frac{\|\mathbf{g}_N\|^2}{\sigma_N^2}+\frac{\|\mathbf{g}_P\|^2}{\sigma_P^2}\right). \tag{45}$$

and where χ_1^2 denotes the central Chi 2 distribution with one degree of freedom. Note that, given some target false alarm and detection probabilities, parameter λ can be computed using the numerical algorithm propose in [8].

5. Minimum SNR expressions

From equation (45) and according to the corresponding model, we derive closed form expressions of the SNR.

5.1. Conventional model

The parameters of equation (45) are given by $\mathbf{g}_N = \mathbf{D}\mathbf{f}_A$, $\mathbf{g}_P = \mathbf{D}\mathbf{f}_B$, $\sigma_N^2 = \sigma_{\mathbf{v}}^2$ and $\sigma_P^2 = \sigma_{\mathbf{w}}^2$. Hence

$$\lambda = 2\delta_0^2\left(\frac{\|\mathbf{D}\mathbf{f}_A\|^2}{\sigma_{\mathbf{v}}^2}+\beta_c^2\frac{\left\|\mathbf{D}^T\mathbf{f}_B\right\|^2}{\sigma_{\mathbf{w}}^2}\right). \tag{46}$$

By letting $\kappa = \frac{\sigma_{\mathbf{v}}^2}{\sigma_{\mathbf{w}}^2}$ and $\mathrm{SNR} = \frac{\|\mathbf{f}_A\|^2}{\sigma_{\mathbf{w}}^2}$, one obtains

$$\lambda = 2\delta_0^2 \mathrm{SNR} \left(\frac{\|\mathbf{D}\mathbf{f}_A\|^2}{\kappa \|\mathbf{f}_A\|^2} + \beta_c^2 \frac{\left\|\mathbf{D}^T\mathbf{f}_B\right\|^2}{\|\mathbf{f}_A\|^2} \right) \tag{47}$$

finally

$$\delta_0 = \sqrt{\frac{\lambda \|\mathbf{f}_A\|^2}{2\mathrm{SNR}\left(\frac{1}{\kappa}\|\mathbf{D}\mathbf{f}_A\|^2 + \beta_c^2 \|\mathbf{D}^T\mathbf{f}_B\|^2\right)}} \tag{48}$$

and the minimum SNR_{min} to resolve the two closely space sources can be given by

$$\mathrm{SNR}_{min} = \frac{\lambda \|\mathbf{f}_A\|^2}{2\delta_0^2\left(\frac{1}{\kappa}\|\mathbf{D}\mathbf{f}_A\|^2 + \beta_c^2 \|\mathbf{D}^T\mathbf{f}_B\|^2\right)} \tag{49}$$

5.2. Time reversal model

In this case, the parameters of equation (45) are given by $\sigma_N^2 = \sigma_v^2$, $\sigma_P^2 = \sigma^2$, $\mathbf{g}_N = \mathbf{D}\mathbf{f}_A$ and $\mathbf{g}_P = \beta_{TR}\left(\mathbf{W}_0\mathbf{H}_d - \frac{\beta_{TR}^2\sigma_{\mathbf{v}}^2}{2\sigma^2}\mathbf{W}_0^{\frac{3}{2}}\mathbf{H}_d\mathbf{W}_0^{\frac{3}{2}}\mathbf{H}_c\right)\mathbf{f}_A^*$. In the following, we have $\mathbf{W}_0 = \sigma\mathbf{R}_0^{-\frac{1}{2}}$, $\mathbf{R}_0 = \sigma_{\mathbf{w}}^2\mathbf{C}_0$ where $\mathbf{C}_0 = \beta_{TR}^2\kappa\mathbf{H}_c + \mathbf{I}$ and $\kappa = \frac{\sigma_{\mathbf{v}}^2}{\sigma_{\mathbf{w}}^2}$. Under theses definitions, equation (45) becomes

$$\lambda = 2\delta_0^2 \frac{\mathrm{SNR}}{\|\mathbf{f}_A\|^2}\left(\frac{1}{\kappa}\|\mathbf{D}\mathbf{f}_A\|^2 + \beta_{TR}^2\left\|\left(\mathbf{C}_0^{-\frac{1}{2}}\mathbf{H}_d - \kappa\,\frac{\beta_{TR}^2}{2}\mathbf{C}_0^{-\frac{3}{4}}\mathbf{H}_d\mathbf{C}_0^{-\frac{3}{4}}\mathbf{H}_c\right)\mathbf{f}_A^*\right\|^2\right) \tag{50}$$

where $\mathrm{SNR} = \frac{\|\mathbf{f}_A\|^2}{\sigma_{\mathbf{w}}^2}$ and

$$\begin{aligned}
\beta_{TR}^2 &= \frac{\|\mathbf{f}_A\|^2}{\|\mathbf{r}^*\|^2} = \frac{\|\mathbf{f}_A\|^2}{\left\|\sum_{l=1}^{L}\mathbf{A}_l^*\mathbf{f}^*\right\|^2 + QN\sigma_v^2} \\
&= \frac{\|\mathbf{f}_A\|^2}{\|\mathbf{A}_{cc}^*\mathbf{f}_A^* + \delta\mathbf{D}\mathbf{f}_A^*\|^2 + QN\sigma_v^2} \qquad (51) \\
&\approx \frac{\|\mathbf{f}_A\|^2}{\|\mathbf{A}_{cc}^*\mathbf{f}_A^*\|^2 + QN\sigma_{\mathbf{v}}^2} = \frac{1}{\frac{1}{\tilde{\beta}^2} + \kappa\frac{QN}{\mathrm{SNR}}} \qquad (52)
\end{aligned}$$

where $\tilde{\beta}^2 = \frac{\|\mathbf{f}_A\|^2}{\|\mathbf{A}_{cc}^*\mathbf{f}_A^*\|^2}$. In order to keep the second order of equation (50) w.r.t. δ, we have taken the constant term of β_{TR}^2 as shown in equation (52).

Finally, the SRL is given by

$$\delta_0 = \sqrt{\frac{\lambda \left\|\mathbf{f}_A\right\|^2}{2\mathrm{SNR}\left(\frac{1}{\kappa}\left\|\mathbf{D}\mathbf{f}_A\right\|^2 + \beta_{TR}^2 \left\|\left(\mathbf{C}_0^{-\frac{1}{2}}\mathbf{H}_d - \kappa\, \frac{\beta_{TR}^2}{2}\mathbf{C}_0^{-\frac{3}{4}}\mathbf{H}_d\mathbf{C}_0^{-\frac{3}{4}}\mathbf{H}_c\right)\mathbf{f}_A^*\right\|^2\right)}} \tag{53}$$

So, the minimum SNR_{min} to resolve the two closely space sources can be given by

$$\mathrm{SNR}_{min} = \frac{\lambda \left\|\mathbf{f}_A\right\|^2}{2\delta_0^2\left(\frac{1}{\kappa}\left\|\mathbf{D}\mathbf{f}_A\right\|^2 + \beta_{TR}^2 \left\|\left(\mathbf{C}_0^{-\frac{1}{2}}\mathbf{H}_d - \kappa\, \frac{\beta_{TR}^2}{2}\mathbf{C}_0^{-\frac{3}{4}}\mathbf{H}_d\mathbf{C}_0^{-\frac{3}{4}}\mathbf{H}_c\right)\mathbf{f}_A^*\right\|^2\right)} \tag{54}$$

6. Numerical results

In this section, we consider two co-located uniform linear arrays A and B with $P = 15 = N = 15$ sensors. The emitted signals are chosen in such a way they are orthogonal and share the same frequency bandwidth. Here, these signals are given by (according to the phase coding scheme in [4])

$$\left[\mathbf{f}(w_q)\right]_m = e^{\jmath 2\pi \frac{mq}{Q}} f(w_q) \tag{55}$$

where $w_q = q\Delta f$, $\Delta f = \frac{B}{Q}$, $B = 50MHz$ is the frequency bandwidth, $Q = 25$ is the number of frequency bins. $\left[\mathbf{f}(w_q)\right]_m$ stands for the emitted signal from the m^{th} sensor. $f(w_q)$ represents the frequency response of a Linear Frequency Modulated (LFM) signal (see [4] for more details).

In our simulations, we are interested in the angular resolution limit (ARL). For that, arrays A and B illuminate $L = 4$ sources where two of them are in the same vicinity. Their different ranges are $r_1 = 1000$, $r_2 = 1200$, $r_3 = 1600$ and $r_4 = 800$. The attenuation factors are assumed to be real and given by $\alpha_1 = 0.9$, $\alpha_2 = 0.8$, $\alpha_3 = 0.7$ and $\alpha_4 = 0.6$. The central direction of arrival of the two closely spaced sources is $\theta_c = 15^o$ while $\theta_3 = 60^o$ and $\theta_4 = 80^o$ are the directions of arrival of the third and fourth sources, respectively. The probabilities of detection and false alarm are $P_d = 0.99$ and $P_{fa} = 0.01$.

In the first experiment, we compare the ARL for the two considered MIMO systems (conventional and TR). In Figures 3, 4 and 5, the plots represent the SRL δ w.r.t. the central direction θ_c for different values of the parameter $\kappa = \frac{\sigma_{\mathbf{v}}^2}{\sigma_{\mathbf{w}}^2}$. As we can see from Figure 3, when the noise term of the time reversed signal is relatively weak with $\kappa < 1$, the transmit and receive signals at antenna A are well matched and hence the performance of the TR-MIMO radar is superior to that of the conventional MIMO radar which corresponds to the results already obtained in [10]. However, for $\kappa = 1$ (Figure 4), the two configurations lead to approximately the same SRL performance. In Figure 5 we consider the case $\kappa > 1$ for which the TR scheme is significantly degraded (due to the weak matching between the transmitted and received signals at antenna A). In that case, we observe that the conventional MIMO radar outperforms the TR-MIMO w.r.t. the SRL performance.

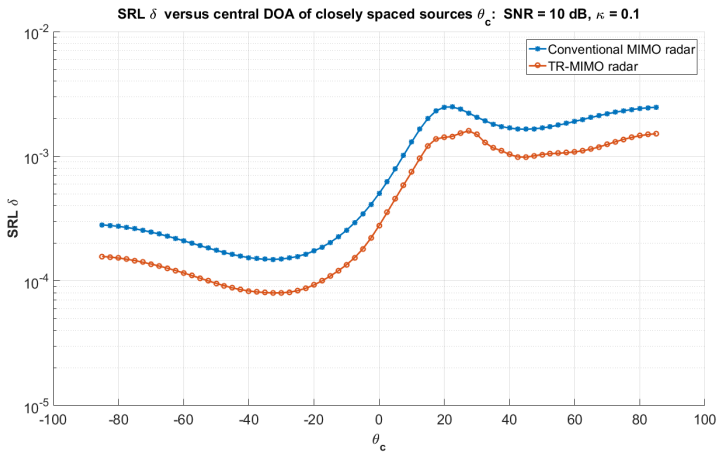

Figure 3: SRL versus θ_c for $\kappa < 1$

To confirm this result, we use now the approximation (simplification) introduced in [4] where the noise term of the time reversed signal is ignored (see equations (37)-(40) in [4]). By considering this simplification, the SRL expres-

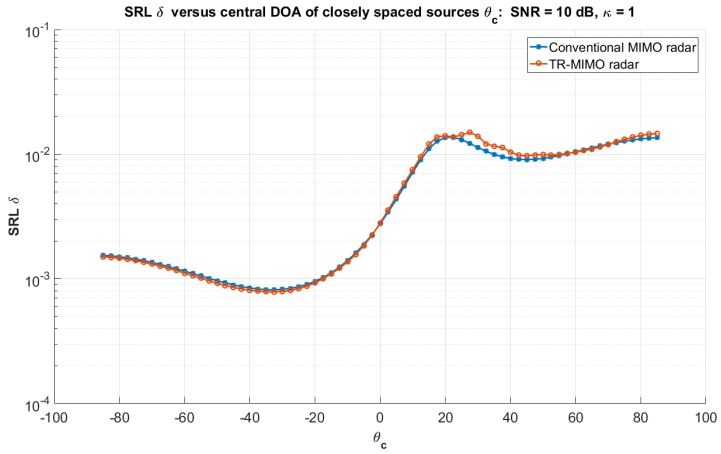

Figure 4: SRL versus θ_c for $\kappa = 1$

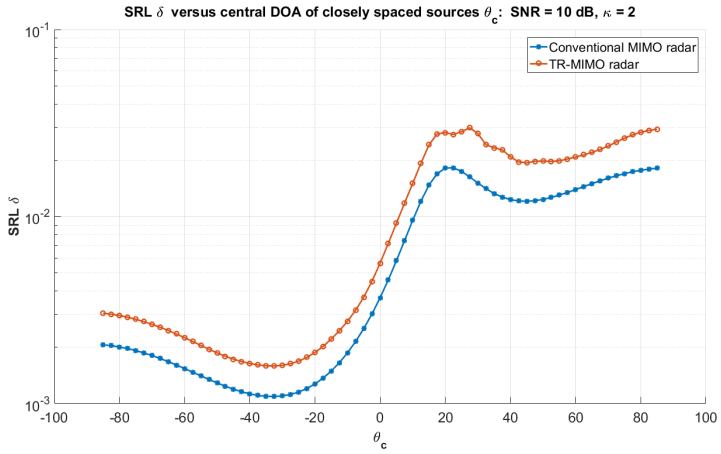

Figure 5: SRL versus θ_c for $\kappa > 1$

sion of the TR-MIMO radar becomes:

$$\delta_0 = \sqrt{\frac{\lambda \left\|\mathbf{f}_A\right\|^2}{2\mathrm{SNR}\left(\frac{1}{\kappa}\left\|\mathbf{D}\mathbf{f}_A\right\|^2 + \beta_{TR}^2 \left\|\mathbf{H}_d \mathbf{f}_A^*\right\|^2\right)}} \tag{56}$$

Figure 6 provides a comparative SRL performance between the conventional and TR schemes with the considered assumption, i.e. eq. (56) for the latter scheme. As we can see, the TR configuration leads to a significant gain as compared to

the conventional configuration when the noise term of the time reversed signal is neglected which confirms the observations of Figures 3, 4 and 5. Another observation made out of this experiment, is the highly nonlinear dependency of the SLR w.r.t. the central direction θ_c as well as the non symmetry of the problem (i.e. the SRL for θ_c is different from the one of $-\theta_c$) which is due to the chosen reference sensor and the non-symmetrical geometry of the considered radar system.

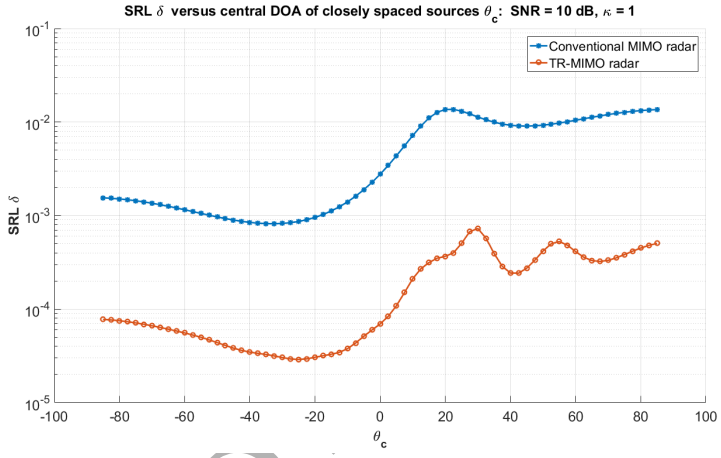

Figure 6: SRL versus θ_c with the simplifying assumption of [4]

In the last experiment, we analyse the SRL and SNR_{min} variations w.r.t. different system parameters. Figure 7, illustrates the variations of the SRL δ versus the SNR for $\kappa = 0.1$ and central DOA $\theta_c = 60^o$. From the plots, one can see that for $\delta = 2.4\ 10^{-4}$, $SNR_{min} = 19$ dB in the conventional MIMO case while $SNR_{min} = 16.5$ for the TR-MIMO case which represents a gain of 2.5 dB. When considering the simplifying assumption of [4] (i.e., by considering the SRL expression given by equation (56)), one can obtain a gain of 7.5 dB for $\delta = 1.97\ 10^{-4}$ as shown in Figure 8.

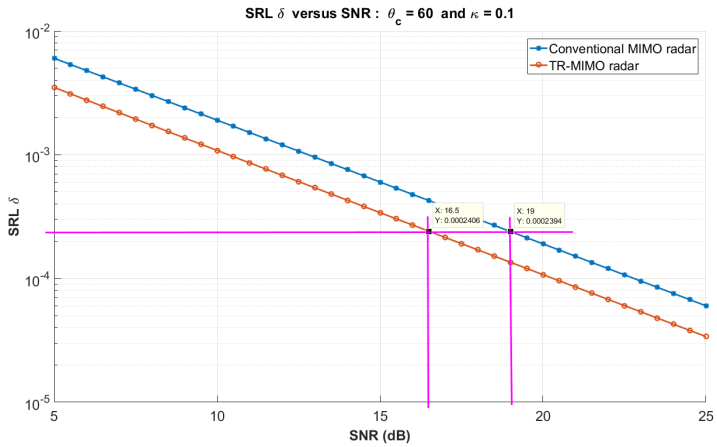

Figure 7: SRL versus θ_c for the considered assumption used in [4]

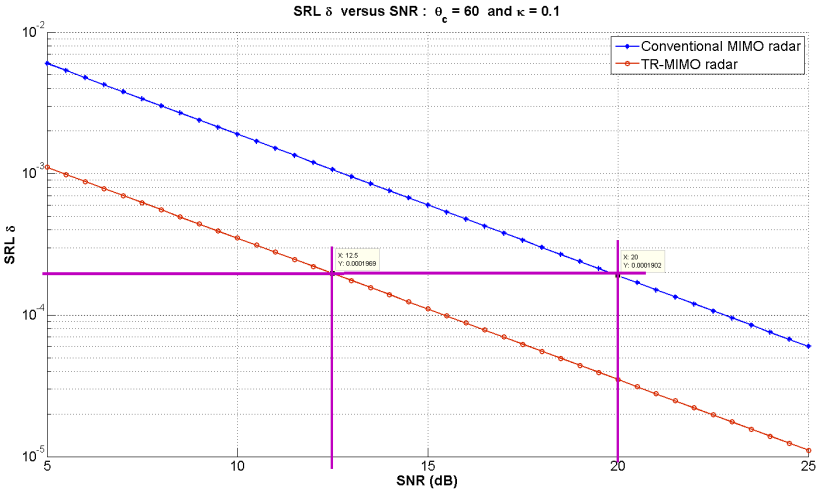

Figure 8: SRL versus θ_c for the considered assumption used in [4]

7. Conclusion

In this paper, we have derived the exact SRL expressions for both TR-MIMO and conventional MIMO radar systems. Based on this study, we have demonstrated that the time reversal can improve the SRL and the obtained gain can be very important in the case where the noise term of the time reversed

signal is weak. Another key observation, is that this gain is highly dependent on the latter assumption and one can obtain better performance results with the conventional scheme if the considered noise in no longer negligible. Also, it is shown that the SRL performance strongly depends on the central direction of arrival of the two closely spaced sources.

Appendices

Appendix A. Taylor expansion of the conventional model

Equation (4) can be expressed as

$$\mathbf{r}(\omega_q) = \left(\mathbf{A}_1(\Omega_1,\omega_q) + \mathbf{A}_2(\Omega_2,\omega_q)\right)\mathbf{f}_A(\omega_q) + \sum_{l=3}^{L}\mathbf{A}_l(\Omega_l,\omega_q)\mathbf{f}_A(\omega_q) + \mathbf{v}(\omega_q). \tag{A.1}$$

and, for n, p, we have

$$\begin{aligned}\left[\mathbf{A}_1(\Omega_1,\omega_q) + \mathbf{A}_2(\Omega_2,\omega_q)\right]_{np} &= \alpha_1 e^{-j(\omega_q+\omega_c)\frac{2r_{0_1}}{c}} e^{-j(\omega_q+\omega_c)(\tau_n^B(\Omega_1)+\tau_p^A(\Omega_1))} \\ &\quad +\alpha_2 e^{-j(\omega_q+\omega_c)\frac{2r_{0_2}}{c}} e^{-j(\omega_q+\omega_c)(\tau_n^B(\Omega_2)+\tau_p^A(\Omega_2))}.\end{aligned} \tag{A.2}$$

where r_{0_i} is the range of source i w.r.t. the reference sensor. Without loss of generality, we assume that Ω_1 and Ω_2 are closely-spaced and $\Omega_3, \cdots, \Omega_L$ are widely spaced (cf. Fig. 1 of [14]). Let us rewrite the angle parameters as

$$\begin{cases} \Omega_1 = \frac{1}{2}(2\Omega_c - \delta) \\ \Omega_2 = \frac{1}{2}(2\Omega_c + \delta) \end{cases} \tag{A.3}$$

Replacing Ω_1, Ω_2, $\tau_n^B(\Omega_l)$ and $\tau_p^A(\Omega_l)$, $l = 1, 2$ by their values in equation (A.2), one obtains

$$\begin{aligned}\left[\mathbf{A}_1(\Omega_1,\omega_q) + \mathbf{A}_2(\Omega_2,\omega_q)\right]_{np} &= e^{-j\frac{(\omega_q+\omega_c)(d_n^B+d_p^A)}{c}\Omega_c}\left[\alpha_1 e^{-j(\omega_q+\omega_c)\frac{2r_{0_1}}{c}} e^{j\frac{(\omega_q+\omega_c)(d_n^B+d_p^A)}{2c}\delta}\right. \\ &+ \left. \alpha_2 e^{-j(\omega_q+\omega_c)\frac{2r_{0_2}}{c}} e^{-j\frac{(\omega_q+\omega_c)(d_n^B+d_p^A)}{2c}\delta}\right].\end{aligned} \tag{A.4}$$

The first-order Taylor expansion is given by

$$\begin{aligned}\left[\mathbf{A}_1(\Omega_1,\omega_q) + \mathbf{A}_2(\Omega_2,\omega_q)\right]_{np} &\overset{1}{\approx} e^{-j\frac{(\omega_q+\omega_c)(d_n^B+d_p^A)}{c}\Omega_c}\left[\alpha_1 e^{-j(\omega_q+\omega_c)\frac{2r_{0_1}}{c}} + \alpha_2 e^{-j(\omega_q+\omega_c)\frac{2r_{0_2}}{c}}\right] \\ &+ j\frac{(\omega_q+\omega_c)(d_n^B+d_p^A)}{2c} e^{-j\frac{(\omega_q+\omega_c)(d_n^B+d_p^A)}{c}\Omega_c}\left[\alpha_1 e^{-j(\omega_q+\omega_c)\frac{2r_{0_1}}{c}} - \alpha_2 e^{-j(\omega_q+\omega_c)\frac{2r_{0_2}}{c}}\right]\delta.\end{aligned} \tag{A.5}$$

By using equations (17)-(20), One can obtain the following matrix form

$$\mathbf{A}_1(\Omega_1,\omega_q)+\mathbf{A}_2(\Omega_2,\omega_q)\overset{1}{\approx}\mathbf{A}_c(\omega_q)+\delta\mathbf{D}(\omega_q). \tag{A.6}$$

and then equation (A.1) becomes

$$\mathbf{r}(\omega_q)=\left(\mathbf{A}_c(\omega_q)+\delta\mathbf{D}(\omega_q)\right)\mathbf{f}_A(\omega_q)+\sum_{l=3}^{L}\mathbf{A}_l(\Omega_l,\omega_q)\mathbf{f}_A(\omega_q)+\mathbf{v}(\omega_q). \tag{A.7}$$

Consequently, one can obtain the first-order Taylor expansion (14)

Appendix B. Taylor expansion of the Time Reversal model

Equation (9) can be written as

$$\begin{aligned}\mathbf{x}(\omega_q) &= \beta_{TR}\left(\mathbf{A}_1^T(\Omega_1,\omega_q)+\mathbf{A}_2^T(\Omega_2,\omega_q)+\sum_{l=3}^{L}\mathbf{A}_l^T(\Omega_l,\omega_q)\right)\\ &\times\left(\mathbf{A}_1^*(\Omega_1,\omega_q)+\mathbf{A}_2^*(\Omega_2,\omega_q)+\sum_{l=3}^{L}\mathbf{A}_l^*(\Omega_l,\omega_q)\right)\mathbf{f}_A^*(\omega_q)\\ &+\beta_{TR}\left(\mathbf{A}_1^T(\Omega_1,\omega_q)+\mathbf{A}_2^T(\Omega_2,\omega_q)+\sum_{l=3}^{L}\mathbf{A}_l^T(\Omega_l)\right)\mathbf{v}^*(\omega_q)+\mathbf{w}(\omega_q).\end{aligned} \tag{B.1}$$

By replacing equation (A.6) in equation (B.1), one obtains

$$\begin{aligned}\mathbf{x}(\omega_q) &= \beta_{TR}\left(\mathbf{A}_{cc}^T(\omega_q)\mathbf{A}_{cc}^*(\omega_q)+\delta\left[\mathbf{A}_{cc}^T(\omega_q)\mathbf{D}^*(\omega_q)+\mathbf{D}^T(\omega_q)\mathbf{A}_{cc}^*(\omega_q)\right]\right)\mathbf{f}_A^*(\omega_q)\\ &+ \beta_{TR}\left(\mathbf{A}_c^T(\Omega_c,\omega_q)+\sum_{l=3}^{L}\mathbf{A}_l^T(\Omega_l)\right)\mathbf{v}^*(\omega_q)+\beta_{TR}\delta\mathbf{D}^T(\omega_q)\mathbf{v}^*(\omega_q)+\mathbf{w}(\omega_q),\\ &= \beta_{TR}\mathbf{H}_c(\omega_q)\mathbf{f}_A^*(\omega_q)+\beta_{TR}\delta\mathbf{H}_d(\omega_q)\mathbf{f}_A^*(\omega_q)+\beta_{TR}\delta\mathbf{D}^T(\omega_q)\mathbf{v}^*(\omega_q)+\mathbf{w}'(\omega_q).\end{aligned} \tag{B.2}$$

where $\mathbf{H}_c(\omega_q)=\mathbf{A}_{cc}^T(\omega_q)\mathbf{A}_{cc}^*(\omega_q)$, $\mathbf{H}_d(\omega_q)=\mathbf{A}_{cc}^T(\omega_q)\mathbf{D}^*(\omega_q)+\mathbf{D}^T(\omega_q)\mathbf{A}_{cc}^*(\omega_q)$, $\mathbf{A}_{cc}(\omega_q)=\mathbf{A}_c(\omega_q)+\sum_{l=3}^{L}\mathbf{A}_l(\Omega_l,\omega_q)$ and $\mathbf{w}'(\omega_q)=\beta_{TR}\mathbf{A}_{cc}^T(\omega_q)\mathbf{v}^*(\omega_q)+\mathbf{w}(\omega_q)$. Consequently, one can obtain the first-order Taylor expansion (23).

Appendix C. Whitening

Let $\mathbf{R}_\delta(\omega_q)$ be the covariance matrix of the noise term $\left(\beta\delta\mathbf{D}^T(\omega_q)\mathbf{v}^*(\omega_q)+\mathbf{w}'(\omega_q)\right)$, the whitening matrix is given by [16, 17]

$$\mathbf{W}_\delta(\omega_q)=\sigma\mathbf{R}_\delta^{-\frac{1}{2}}(\omega_q). \tag{C.1}$$

In this case, the whitened observation vector is given by

$$\begin{aligned}\tilde{\mathbf{x}}(\omega_q) &= \mathbf{W}_\delta(\omega_q)\mathbf{x}(\omega_q),\\ &= \beta\mathbf{W}_\delta(\omega_q)\mathbf{H}_c(\omega_q)\mathbf{f}_A^*(\omega_q) + \beta\delta\mathbf{W}_\delta(\omega_q)\mathbf{H}_d(\omega_q)\mathbf{f}_A^*(\omega_q) + \mathbf{v}'(\omega_q) \quad \text{(C.2)}\end{aligned}$$

where $\mathbf{v}'(\omega_q) = \mathbf{W}_\delta(\omega_q)\left(\beta\delta\mathbf{D}^T(\omega_q)\mathbf{v}^*(\omega_q) + \mathbf{w}'(\omega_q)\right) \sim CN(\mathbf{0}, \sigma^2\mathbf{I})$.

Now, let $\mathbf{R}_0(\omega_q)$ be the covariance matrix of $\left(\beta_{TR}\delta\mathbf{D}^T(\omega_q)\mathbf{v}^*(\omega_q) + \mathbf{w}'(\omega_q)\right)$ for $\delta = 0$ $\left(\text{i.e., } \mathbf{R}_0(\omega_q) = E\left[\mathbf{w}'(\omega_q)\mathbf{w}'^H(\omega_q)\right] = \beta^2\sigma_{\mathbf{v}}^2\mathbf{H}_c(\omega_q) + \sigma_{\mathbf{w}}^2\mathbf{I}\right)$. Let us express $\mathbf{W}_\delta(\omega_q)$ as function of $\mathbf{W}_0(\omega_q) = \sigma\mathbf{R}_0^{-\frac{1}{2}}(w_q)$.

We recall here $\mathbf{R}_\delta(\omega_q) = E\left[\left(\beta\delta\mathbf{D}(\omega_q)\mathbf{v}^*(\omega_q) + \mathbf{w}'(\omega_q)\right)\left(\beta\delta\mathbf{D}(\omega_q)\mathbf{v}^*(\omega_q) + \mathbf{w}'(\omega_q)\right)^H\right]$ and

$$\begin{aligned}\mathbf{R}_\delta(\omega_q) &\overset{1}{\approx} \mathbf{R}_0(\omega_q) + \beta\delta\left(\mathbf{D}^T(\omega_q)E\left[\mathbf{v}^*(\omega_q)\mathbf{w}'^H(\omega_q)\right] + E\left[\mathbf{w}'(\omega_q)\mathbf{v}^T(\omega_q)\right]\mathbf{D}^*(\omega_q)\right), \quad \text{(C.3)}\\ &= \mathbf{R}_0(\omega_q) + \delta\mathbf{R}(\omega_q), \quad \text{(C.4)}\\ &= \mathbf{R}_0(\omega_q)^{\frac{1}{2}}\left(\mathbf{I} + \delta\mathbf{R}_0^{-\frac{1}{2}}(\omega_q)\mathbf{R}(\omega_q)\mathbf{R}_0^{-\frac{1}{2}}(\omega_q)\right)\mathbf{R}_0^{\frac{1}{2}}(\omega_q). \quad \text{(C.5)}\end{aligned}$$

where

$$\begin{aligned}\mathbf{R}(\omega_q) &= \beta\mathbf{D}^T(\omega_q)E\left[\mathbf{v}^*(\omega_q)\mathbf{w}'^H(\omega_q)\right] + \beta E\left[\mathbf{w}'(\omega_q)\mathbf{v}^T(\omega_q)\right]\mathbf{D}^*(\omega_q), \quad \text{(C.6)}\\ &= \beta\mathbf{D}^T(\omega_q)E\left[\mathbf{v}^*(\omega_q)\left(\beta\mathbf{A}_{cc}^T(\omega_q)\mathbf{v}^*(\omega_q) + \mathbf{w}(\omega_q)\right)^H\right]\\ &+ \beta E\left[\left(\beta\mathbf{A}_{cc}^T(\omega_q)\mathbf{v}^*(\omega_q) + \mathbf{w}(\omega_q)\right)\mathbf{v}^T(\omega_q)\right]\mathbf{D}^*(\omega_q), \quad \text{(C.7)}\\ &= \beta\mathbf{D}^T(\omega_q)\left\{E\left[\mathbf{v}^*(\omega_q)\mathbf{v}^T(\omega_q)\right]\beta\mathbf{A}_{cc}^*(\omega_q) + \underbrace{E\left[\mathbf{v}^*(\omega_q)\mathbf{w}^H(\omega_q)\right]}_{0}\right\}\\ &+\beta\left\{\beta\mathbf{A}_{cc}^T(\omega_q)E\left[\mathbf{v}^*(\omega_q)\mathbf{v}^T(\omega_q)\right] + \underbrace{E\left[\mathbf{w}(\omega_q)\mathbf{v}^T(\omega_q)\right]}_{0}\right\}\mathbf{D}^*(\omega_q), \quad \text{(C.8)}\\ &= \beta^2\sigma_{\mathbf{v}}^2\left\{\mathbf{D}^T(\omega_q)\mathbf{A}_{cc}^*(\omega_q) + \mathbf{A}_{cc}^T(\omega_q)\mathbf{D}^*(\omega_q)\right\}, \quad \text{(C.9)}\\ &= \beta^2\sigma_{\mathbf{v}}^2\mathbf{H}_d(\omega_q). \quad \text{(C.10)}\end{aligned}$$

and hence

$$\mathbf{R}_\delta(\omega_q) = \beta^2\sigma_{\mathbf{v}}^2\left(\mathbf{H}_c(\omega_q) + \delta\mathbf{H}_d(\omega_q)\right) + \sigma_{\mathbf{w}}^2\mathbf{I}. \quad \text{(C.11)}$$

equation (C.5) leads to the following first-order Taylor expansion

$$\mathbf{R}_{\delta}^{-\frac{1}{2}}(\omega_q) = \mathbf{R}_0^{-\frac{1}{2}}(\omega_q) - \frac{1}{2}\delta\mathbf{R}_0^{-\frac{3}{4}}(\omega_q)\mathbf{R}(\omega_q)\mathbf{R}_0^{-\frac{3}{4}}(\omega_q). \tag{C.12}$$

and thus

$$\mathbf{W}_{\delta}(\omega_q) = \mathbf{W}_0(\omega_q) - \frac{1}{2}\delta\mathbf{W}_0^{\frac{3}{2}}(\omega_q)\frac{1}{\sigma^2}\mathbf{R}(\omega_q)\mathbf{W}_0^{\frac{3}{2}}(\omega_q). \tag{C.13}$$

Now, we replace $\mathbf{W}_{\delta}(\omega_q)$ and $\mathbf{R}(\omega_q)$ by their expressions in equation (C.2), one can obtain (27).

Appendix D. Statistic of T(z)

We recall that under hypothesis $\mathcal{H}_1$

$$\mathbf{z} = \begin{bmatrix} \mathbf{z}_N \\ \mathbf{z}_P \end{bmatrix} = \delta \begin{bmatrix} \mathbf{g}_N \\ \mathbf{g}_P \end{bmatrix} + \begin{bmatrix} \xi_N \\ \xi_P \end{bmatrix}. \tag{D.1}$$

hence $\mathbf{z}_N = \delta\mathbf{g}_N + \xi_N$ and $\mathbf{z}_P = \delta\mathbf{g}_P + \xi_P$. We assume ξ_N and ξ_P are two circular complex white Gaussian vectors according to

$$\Re(\xi_N) \sim \mathcal{N}(0, \frac{\sigma_N^2}{2}\mathbf{I}), \qquad \Im(\xi_N) \sim \mathcal{N}(0, \frac{\sigma_N^2}{2}\mathbf{I}), \tag{D.2}$$

$$\Re(\xi_P) \sim \mathcal{N}(0, \frac{\sigma_P^2}{2}\mathbf{I}), \qquad \Im(\xi_P) \sim \mathcal{N}(0, \frac{\sigma_P^2}{2}\mathbf{I}). \tag{D.3}$$

we have $\mathbf{z}_N \sim \mathcal{N}(\delta\mathbf{g}_N, \sigma_N^2\mathbf{I})$ since

$$\begin{aligned} E(\mathbf{z}_N) &= E(\Re(\mathbf{z}_N)) + \jmath E(\Im(\mathbf{z}_N)), & \text{(D.4)}\\ &= \delta\Re(\mathbf{g}_N) + \jmath\delta\imath(\mathbf{g}_N), & \text{(D.5)}\\ &= \delta\mathbf{g}_N. & \text{(D.6)} \end{aligned}$$

Using the circular property of ξ_N

$$\begin{aligned} E\left((\mathbf{z}_N - \delta\mathbf{g}_N)(\mathbf{z}_N - \delta\mathbf{g}_N)^H\right) &= E(\xi_N\xi_N^H), & \text{(D.7)}\\ &= E(\Re(\xi_N)\Re(\xi_N)^T) + E(\Im(\xi_N)\Im(\xi_N)^T), & \text{(D.8)}\\ &= (\frac{\sigma_N^2}{2} + \frac{\sigma_N^2}{2})\mathbf{I}, & \text{(D.9)}\\ &= \sigma_N^2\mathbf{I}. & \text{(D.10)} \end{aligned}$$

By following the same way, we have $\mathbf{z}_P \sim \mathcal{N}(\delta\mathbf{g}_P, \sigma_P^2\mathbf{I})$. Let

$$u = \frac{1}{\sigma_N^2}\Re(\mathbf{g}_N^H\mathbf{z}_N), \tag{D.11}$$

$$v = \frac{1}{\sigma_P^2}\Re(\mathbf{g}_P^H\mathbf{z}_P). \tag{D.12}$$

we have

$$E(u) = E\left(\frac{1}{\sigma_N^2}\left(\Re(\mathbf{g}_N)^T\Re(\mathbf{z}_N) + \Im(\mathbf{g}_N)^T\Im(\mathbf{z}_N)\right)\right), \tag{D.13}$$

$$= \frac{1}{\sigma_N^2}\left[\Re(\mathbf{g}_N)^T E(\Re(\mathbf{z}_N)) + \Im(\mathbf{g}_N)^T E(\Im(\mathbf{z}_N))\right], \tag{D.14}$$

$$= \frac{1}{\sigma_N^2}\left[\delta\left\|\Re(\mathbf{g}_N)\right\|^2 + \delta\left\|\Im(\mathbf{g}_N)\right\|^2\right], \tag{D.15}$$

$$= \frac{\delta\left\|\mathbf{g}_N\right\|^2}{\sigma_N^2} \tag{D.16}$$

and

$$C_u = E\left(\left(u - \frac{\delta\left\|\mathbf{g}_N\right\|^2}{\sigma_N^2}\right)^2\right) = \frac{1}{\sigma_N^4}E\left(\left(\Re(\mathbf{g}_N^H\mathbf{z}_N) - \delta\left\|\mathbf{g}_N\right\|^2\right)^2\right),$$

$$= \frac{1}{\sigma_N^4}E\left(\Re^2\left(\mathbf{g}_N^H(\mathbf{z}_N - \delta\mathbf{g}_N)\right)\right), \tag{D.17}$$

$$= \frac{1}{\sigma_N^4}E\left(\Re^2\left(\mathbf{g}_N^H\xi_N\right)\right), \tag{D.18}$$

$$= \frac{1}{\sigma_N^4}E\left(\left(\Re(\mathbf{g}_N)^T\Re(\xi_N) + \Im(\mathbf{g}_N)^T\Im(\xi_N)\right)^2\right), \tag{D.19}$$

$$= \frac{1}{\sigma_N^4}\frac{\sigma_N^2}{2}\left\|\mathbf{g}_N\right\|^2, \tag{D.20}$$

$$= \frac{1}{2\sigma_N^2}\left\|\mathbf{g}_N\right\|^2. \tag{D.21}$$

Thus

$$u \sim \mathcal{N}\left(\frac{\delta\left\|\mathbf{g}_N\right\|^2}{\sigma_N^2}, \frac{\left\|\mathbf{g}_N\right\|^2}{2\sigma_N^2}\right), \tag{D.22}$$

$$v \sim \mathcal{N}\left(\frac{\delta\left\|\mathbf{g}_P\right\|^2}{\sigma_P^2}, \frac{\left\|\mathbf{g}_P\right\|^2}{2\sigma_P^2}\right) \tag{D.23}$$

The statistic of $u + v$ is

$$\mathcal{CN}\left(\delta\left(\frac{\left\|\mathbf{g}_N\right\|^2}{\sigma_N^2} + \frac{\left\|\mathbf{g}_P\right\|^2}{\sigma_P^2}\right), \frac{1}{2}\left(\frac{\left\|\mathbf{g}_N\right\|^2}{\sigma_N^2} + \frac{\left\|\mathbf{g}_P\right\|^2}{\sigma_P^2}\right)\right)$$

if u and v are independent random variables.

Now, we can verify the following equality:

$$\mathbf{T}(\mathbf{z}) = \frac{(u+v)^2}{C_{u+v}}, \tag{D.24}$$

$$= \frac{2\sigma_N^2\sigma_P^2}{\sigma_N^2\left\|\mathbf{g}_P\right\|^2+\sigma_P^2\left\|\mathbf{g}_N\right\|^2}\Re^2\left(\frac{1}{\sigma_N^2}\mathbf{g}_N^H\mathbf{z}_N+\frac{1}{\sigma_P^2}\mathbf{g}_P^H\mathbf{z}_P\right). \tag{D.25}$$

The non-centrality parameter is

$$\lambda = \frac{E^2(u+v)}{C_{u+v}} = 2\delta^2\left(\frac{\left\|\mathbf{g}_N\right\|^2}{\sigma_N^2}+\frac{\left\|\mathbf{g}_P\right\|^2}{\sigma_P^2}\right). \tag{D.26}$$

and

$$\mathbf{T}(\mathbf{z}) \sim \chi_1^2(\lambda).$$

References

[1] F. Foroozan, A. Asif, Time reversal based active array source localization, IEEE Transactions on Signal Processing 59 (2011) 210–225.

[2] Pengcheng Gong, Wen-Qin Wang, Xianrong Wan, Adaptive weight matrix design and parameter estimation via sparse modeling for MIMO radar, Signal Processing 139 (2017) 1–11.

[3] J. Li, P. Stoica, MIMO Radar Signal Processing, John Wiley and Sons, Inc, 2009.

[4] J. Yuanwei, J.M.F. Moura, N. O'Donoughue, Time reversal in multiple-input multiple-output radar, IEEE Journal of Selected Topics in Signal Processing 4 (2010) 210–225.

[5] A.J. Den Dekker, A. Van Den Bos, Resolution, a survey, Journal of the Optical Society of America 14 (1997) 547–557.

[6] M.N. El Korso, R. Boyer, A. Renaux, S. Marcos, Statistical analysis of achievable resolution limit in the near field source localization context, Signal Processing 92 (2012) 547 – 552.

[7] S.T. Smith, Statistical resolution limits and the complexified Cramér Rao Bound, IEEE Transactions on Signal Processing 53 (2005) 1597–1609.

[8] Z. Liu, A. Nehorai, Statistical angular resolution limit for point sources, IEEE Transactions on Signal Processing 55 (2007) 5521–5527.

[9] R. Boyer, Performance bounds and angular resolution limit for the moving colocated MIMO radar, IEEE Transactions on Signal Processing 59 (2011) 1539–1552.

[10] F. Foroozan, A. Asif, R. Boyer, Time Reversal MIMO Radar : Improved CRB and Angular Resolution Limit, In Proceedings: International Conference on Acoustics, Speech and Signal Processing (ICASSP) (2013) 4125–4129.

[11] M.N. El Korso, R. Boyer, A. Renaux, S. Marcos, Statistical resolution limit for source localization with clutter interference in a MIMO radar context, IEEE Transactions on Signal Processing 60 (2012) 987–992.

[12] Yuanwei Jin, Jose M.F. Moura, Asymptotic noise analysis of time reversal detection, In Proceedings: Fortieth Asilomar Conference on Signals, Systems and Computers, DOI: 10.1109/ACSSC.2006.354853.

[13] Jose M. F. Moura ; Yuanwei Jin, Detection by time reversal: Single antenna, IEEE Transactions on Signal Processing 55 (2007) 187 – 201.

[14] M.N. El Korso, R. Boyer, A. Renaux, S. Marcos, On the asymptotic resolvability of two point sources in known subspace interference using a GLRT-based framework, Signal Processing 92 (2012) 2471–2483.

[15] S. Kay, Fundamentals of Statistical Signal Processing, Volume II: Detection Theory, Prentice Hall, 1998.

[16] X.L. Zhu, X. Zhang, Y. Jimin, Natural gradient-based recursive least-squares algorithm for adaptive blind source separation, Science in China 47 (2004) 55–65.

[17] A. Belouchrani, K. Abed-Meraim, J.F. Cardoso, E. Moulines, A blind source separation technique using second-order statistics, IEEE Transactions on Signal Processing 45 (1997) 434–444.